

## **Electronic Supplementary Information**

**Neutral ligand TIPA-based two 2D metal-organic frameworks:  
ultrahigh selectivity of C<sub>2</sub>H<sub>2</sub>/CH<sub>4</sub> and efficient sensing and sorption of  
Cr(VI)**

Hong-Ru Fu, Ying Zhao, Zhan Zhou, Xiao-Gang Yang, Lu-Fang Ma\*

<sup>a</sup>College of Chemistry and Chemical Engineering, Henan Province Function-oriented  
Porous Materials Key Laboratory, Luoyang Normal University, Luoyang, 471934  
Henan, P. R. China.

\* Corresponding Author  
Email: mazhuxp@126.com

## Materials and measurements

All reagents and solvents employed were commercially available. Powder X-ray diffraction (PXRD) patterns were collected on a MiniFlex-II diffractometer using Cu ( $\lambda = 1.54178 \text{ \AA}$ ) radiation with a speed of  $2^\circ/\text{min}$ . Thermogravimetric analysis (TG) was performed on a Netzsch STA449C equipped with a platinum pan and heated at a rate of  $5^\circ\text{C}/\text{min}$  in air.  $\text{CO}_2$  (99.99%),  $\text{N}_2$  (99.99%),  $\text{CH}_4$  (99.99%) and  $\text{C}_2\text{H}_2$  (99.99%) gas adsorption measurements were performed using an ASAP 2020 system. Elemental analyses of C, N, and H were performed on a Vario EL III elemental analyzer. Fluorescence spectra for the compounds were collected on F-7000 FL Spectrophotometer equipped with a 150 W xenon lamp as the excitation source at room temperature. UV-visible absorption and emission spectra were recorded on a Lambda 750s UV-vis spectrophotometer. The infrared spectrum was measured with KBr pellets in the  $4000\text{--}400 \text{ cm}^{-1}$  region on a Nicolet 170SX spectrometer.

## Powder X-ray Diffraction Studies

X-ray powder diffraction (XPD) patterns of **1** and **2** was collected on a MiniFlex-II diffractometer.

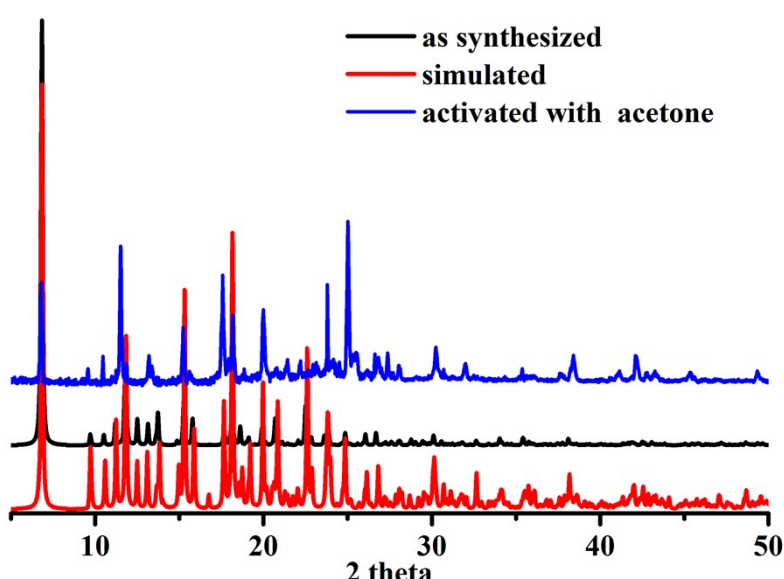


**Figure. S1** PXRD patterns of as-synthesized **1** as well as samples treated in the

acetone solution.

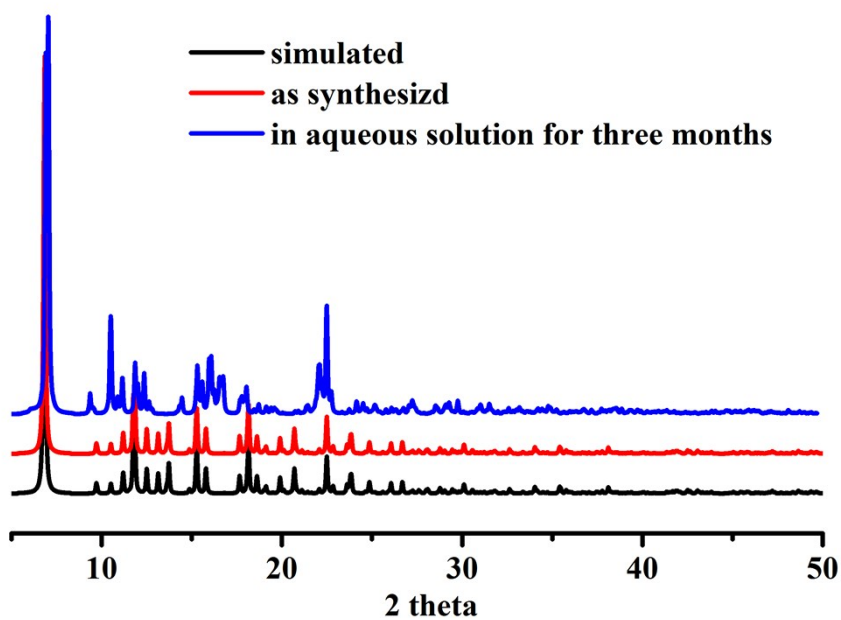


**Figure. S2** PXRD patterns of as-synthesized **2** as well as samples treated in water solution.

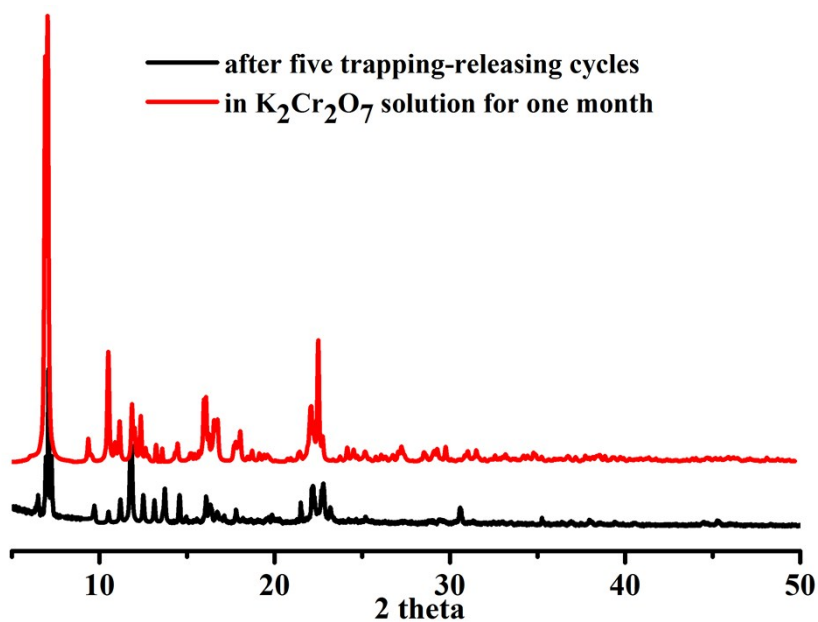


**Figure. S3** PXRD patterns of as-synthesized **2** as well as samples treated in corresponding solution.

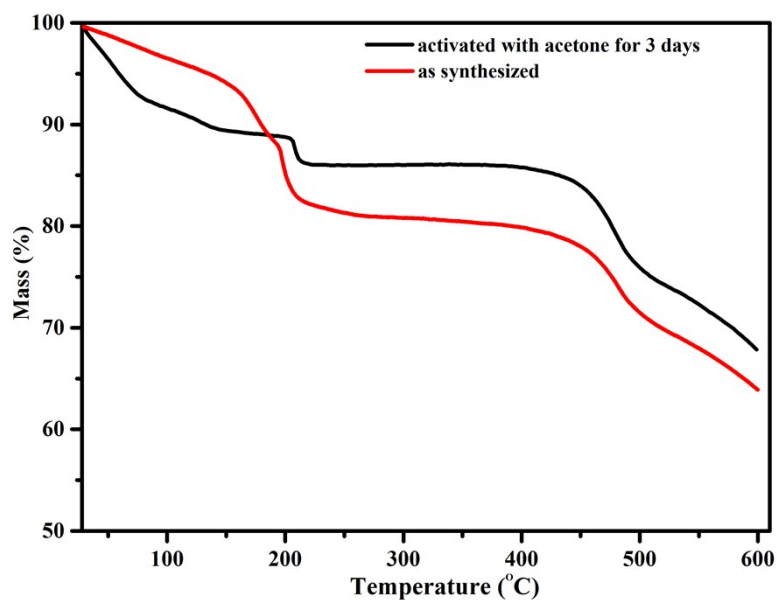


**Figure. S4** TGA curves of compound **1** under nitrogen gas atmosphere.

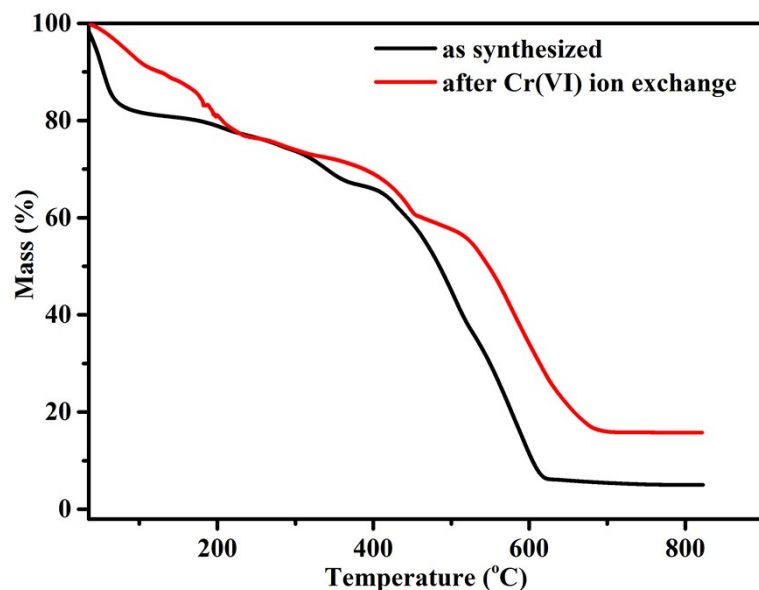


**Figure. S5** TGA curves of compound **2** under air atmosphere.

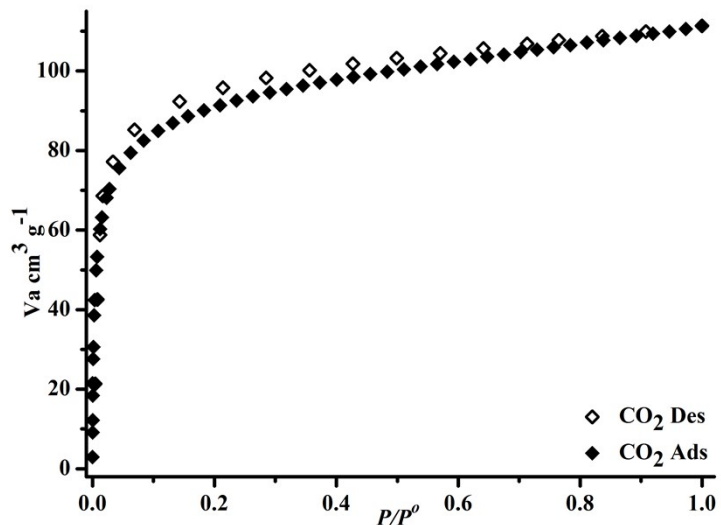


**Figure. S6** CO<sub>2</sub> sorption isotherms of compound **1** at 195 K.

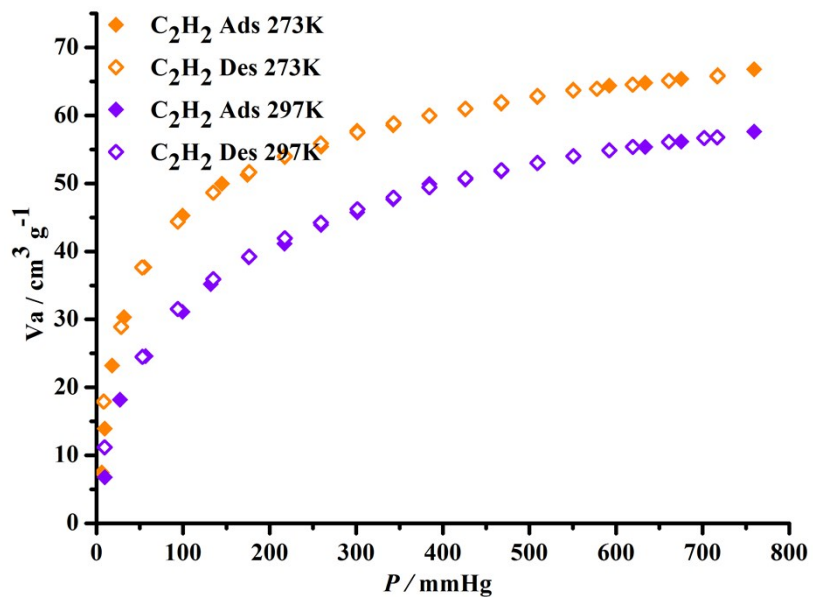


**Figure. S7** C<sub>2</sub>H<sub>2</sub> sorption isotherms of compound **1** at 273 and 297 K, respectively.

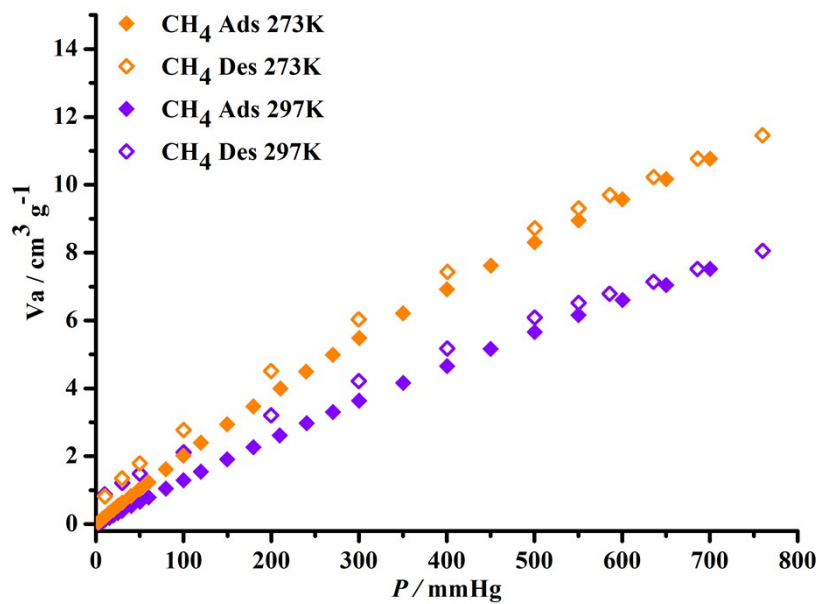


**Figure. S8** CH<sub>4</sub> sorption isotherms of compound 1 at 273 and 297 K, respectively.

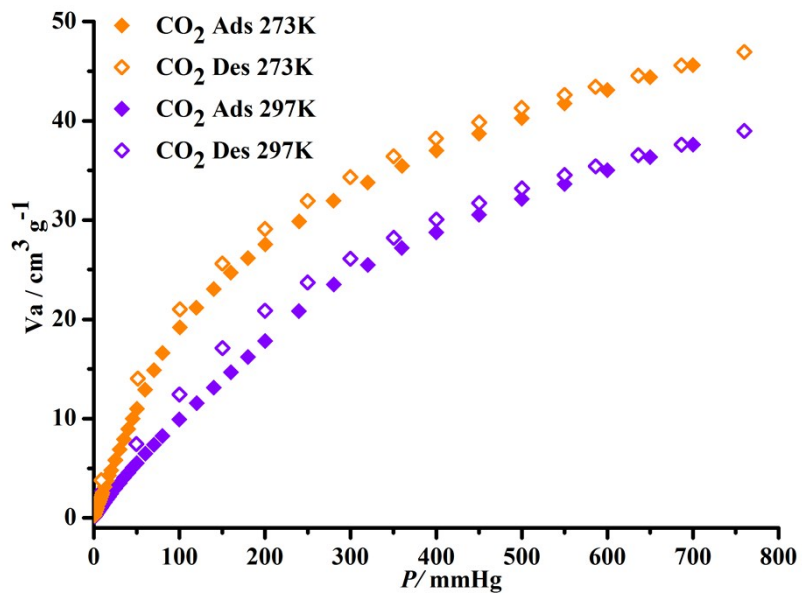


**Figure. S9** CO<sub>2</sub> sorption isotherms of compound 1 at 273 and 297 K, respectively.

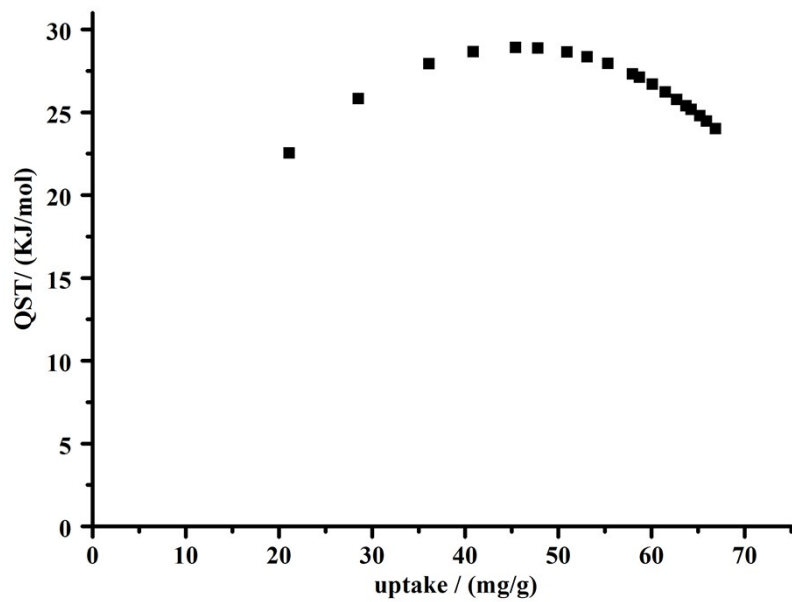


**Figure. S10** The enthalpies ( $Q_{st,n=0}$ /kJ mol<sup>-1</sup>) of C<sub>2</sub>H<sub>2</sub> on complex **1** at 273 and 297 K obtained from the virial equation.

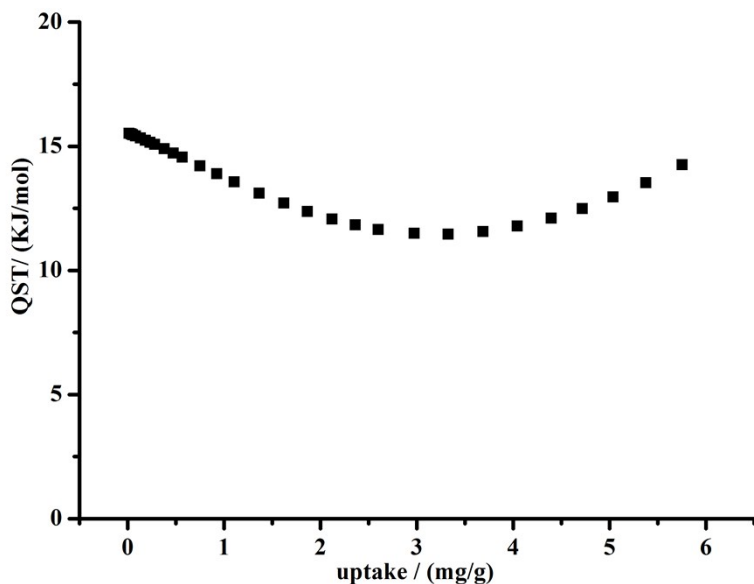


**Figure. S11** The enthalpies ( $Q_{st,n=0}$ /kJ mol<sup>-1</sup>) of CH<sub>4</sub> on complex **1** at 273 and 297 K obtained from the virial equation.

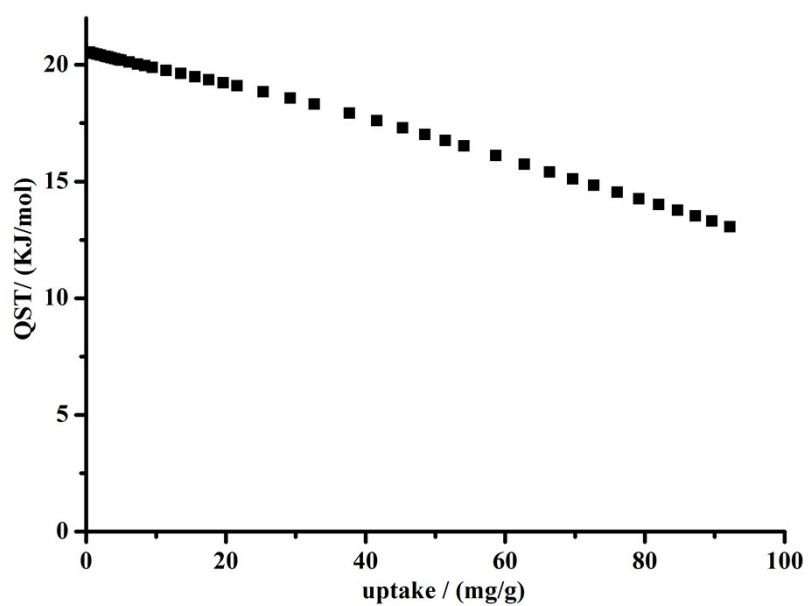


**Figure. S12** The enthalpies ( $Q_{st,n=0}/\text{kJ mol}^{-1}$ ) of  $\text{CO}_2$  on complex **1** at 273 and 297 K obtained from the virial equation.

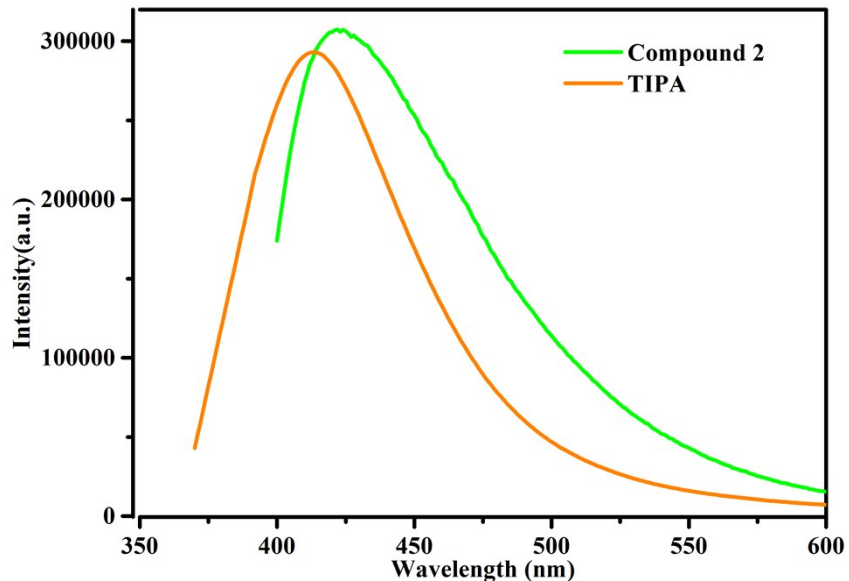


**Figure. S13** The fluorescence spectra for **2** and TIPA.

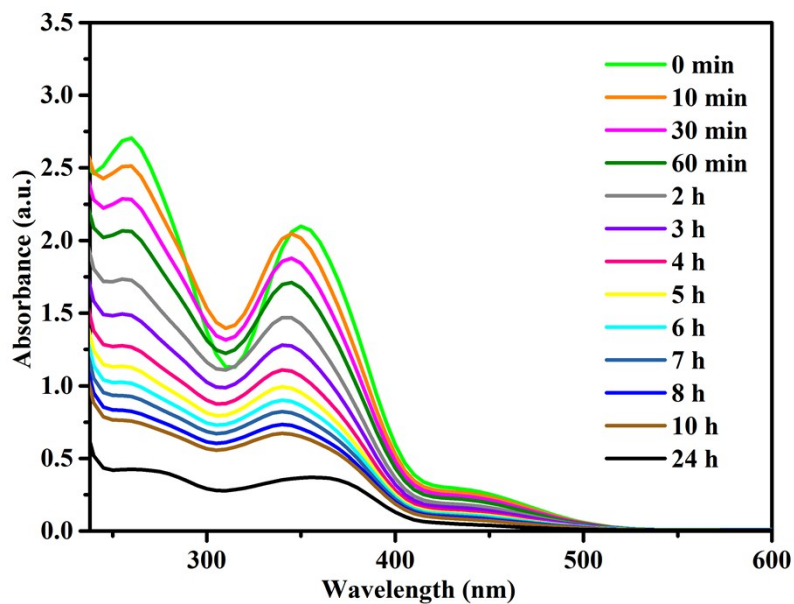


**Figure. S14** UV-vis adsorption spectra of chromate exchange solution on **2**, the exchange process carried out at  $2 \times 10^{-3}$  mol L<sup>-1</sup>, the Cr(VI) was thoroughly adsorbed after 24 h.

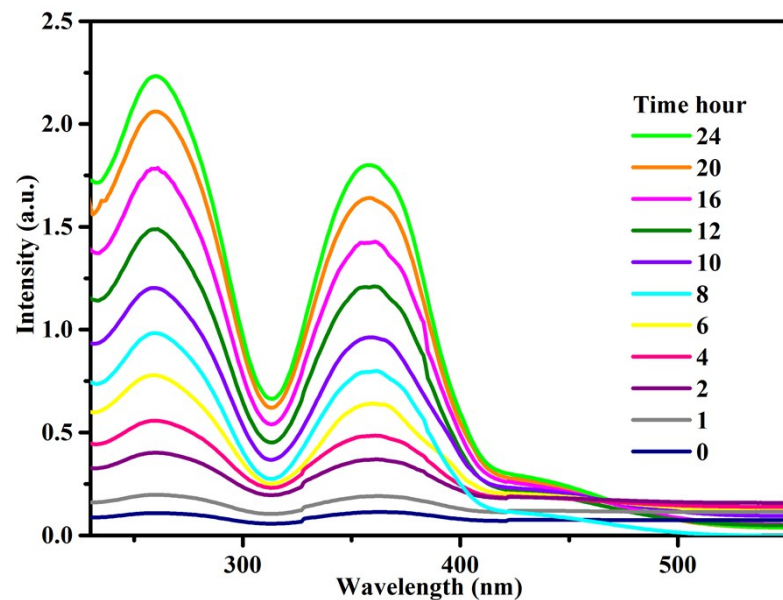


**Figure. S15** UV-vis adsorption spectra of chromate exchange solution on **2**, the exchange process carried out at  $2 \times 10^{-3}$  mol L<sup>-1</sup>, the Cr(VI) was thoroughly desorbed after 24 h.

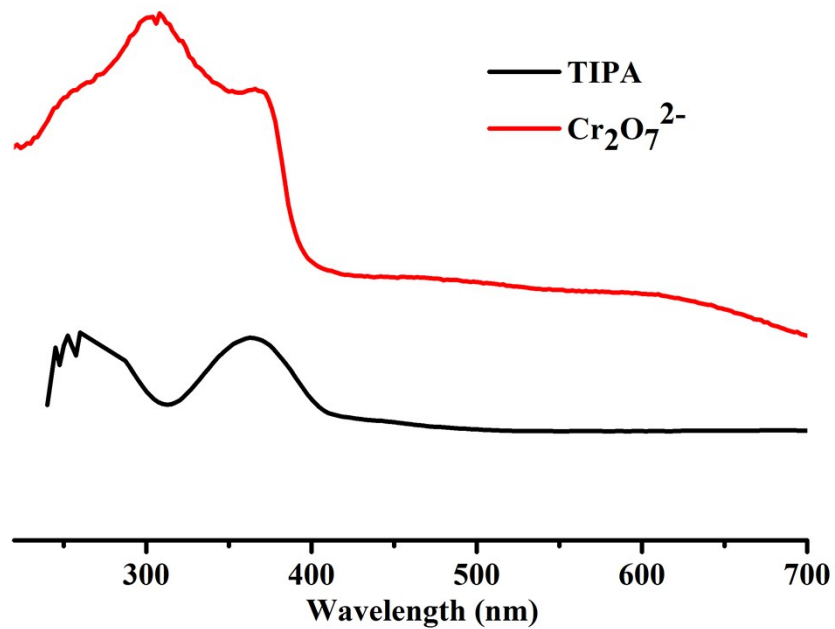


**Figure. S16** UV-vis absorption spectrum of TIPA and  $\text{Cr}_2\text{O}_7^{2-}$  in aqueous solution.

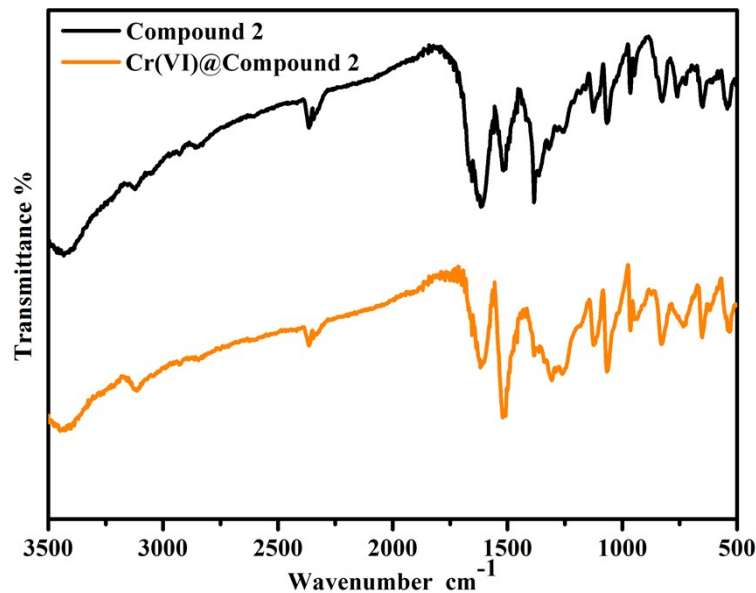


**Figure. S17** IR spectra for: (a) as-synthesized **2** (black curve); (b) **2** containing  $\text{Cr}_2\text{O}_7^{2-}$  obtained in a  $2 \times 10^{-3}$  mol  $\text{L}^{-1}$   $\text{K}_2\text{Cr}_2\text{O}_7$  aqueous solution for 72 hours. The peaks of  $\text{ClO}_4^-$  significantly reduced, even disappeared, indicating that the  $\text{ClO}_4^-$  ions were replaced by  $\text{Cr}_2\text{O}_7^{2-}$  anion ions (orange curve).

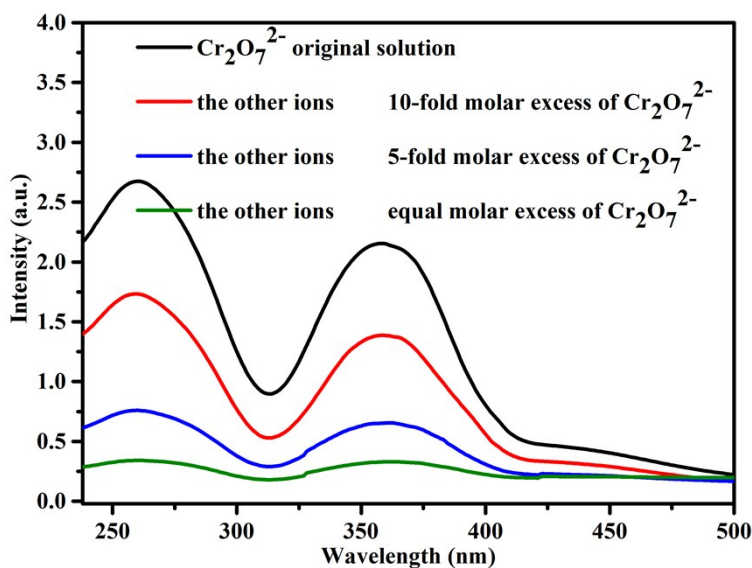


**Figure. 18** The UV-vis absorbance spectra of  $\text{Cr}_2\text{O}_7^{2-}$  on the selective trapping of **1**. a) The  $\text{Cr}_2\text{O}_7^{2-}$  UV-vis absorbance spectra of the mixed solution containing  $\text{Cl}^-$ ,  $\text{Br}^-$ ,  $\text{NO}_3^-$  equal-fold molar excess of  $\text{Cr}_2\text{O}_7^{2-}$  after 24 hours (green line); b) The  $\text{Cr}_2\text{O}_7^{2-}$  UV-vis absorbance spectra of the mixed solution containing  $\text{Cl}^-$ ,  $\text{Br}^-$ ,  $\text{NO}_3^-$  5-fold molar excess of  $\text{Cr}_2\text{O}_7^{2-}$  after 24 hours (blue line); c) The  $\text{Cr}_2\text{O}_7^{2-}$  UV-vis absorbance spectra of the mixed solution containing  $\text{Cl}^-$ ,  $\text{Br}^-$ ,  $\text{NO}_3^-$ ,  $\text{SO}_4^{2-}$ ,  $\text{ClO}_4^-$  and  $\text{BF}_4^-$  10-fold molar excess of  $\text{Cr}_2\text{O}_7^{2-}$  after 24 hours (red line); The  $\text{Cr}_2\text{O}_7^{2-}$  UV-vis absorbance spectra of  $10 \times 10^{-3}$  mol  $\text{L}^{-1}$   $\text{Cr}_2\text{O}_7^{2-}$  solution (black line).

**Table. S1** Comparison of chromate detection limits among MOF.

MOFs	Detection limit	Ref.
$[\text{Eu}_7(\text{mtb})_5(\text{H}_2\text{O})_{16}] \cdot \text{NO}_3 \cdot 8\text{DMA} \cdot 18\text{H}_2\text{O}$	0.56 ppb	1
$\text{Eu}^{3+}@\text{MIL-124}$	7.8 ppb	2
$[\text{Cd}(\text{TIPA})](\text{ClO}_4)_2$	8.0 ppb	This work
$[\text{Ag}(\text{m3-abtz})] \cdot (\text{NO}_3) \cdot (0.125\text{H}_2\text{O})$	9.88 ppb	3
$[\text{Zn}_7(\text{TPPE})_2(\text{SO}_4^{2-})_7](\text{DMF} \cdot \text{H}_2\text{O})$	27.0 ppb	4
$[\text{Eu}_2\text{L}1.5(\text{H}_2\text{O})2\text{EtOH}] \cdot \text{DMF}$	0.52 ppm	5
$[\text{Zn}(\text{btz})]\text{n}$	0.52 ppm	6
$[\text{Ln}(\text{Hpzbc})_2(\text{NO}_3)] \cdot \text{H}_2\text{O}$	1.04 ppm	7

## References

- 1 W. Liu, Y. L. Wang, Z. L. Bai, Y. X. Li, Y. X. Wang, L. H. Chen, L. Xu, J. Diwu, Z. F. Chai, S. A. Wang, *ACS Appl. Mater. Interfaces*, 2017, **9**, 16448–16457.
- 2 Y. L. Ying, Y. Liu, X. Y. Wang, Y. Y. Mao, W. Cao, P. Hu, X. S. Peng, *ACS Appl. Mater. Interfaces*, 2015, **7**, 721–729.
- 3 B. Ding, C. Guo, S. X. Liu, Y. Cheng, X. X. Wu, X. M. Su, Y. Y. Liu, Y. Li, *RSC Adv.*, 2016, **6**, 33888–33900.
- 4 X. X. Wu, H. R. Fu, M. L. Han, Z. Zhou, L. F. Ma, *Cryst. Growth Des.*, 2017, **17**, 6041–6048.
- 5 W. Liu, X. Huang, C. Xu, C. Chen, L. Yang, W. Dou, W. Chen, H. Yang, W. Liu, *Chem. Eur. J.*, 2016, **22**, 18769–18776.
- 6 C. S. Cao, H. C. Hu, H. Xu, W. Z. Qiao, B. Zhao, *CystEngComm*, 2016, **18**, 4445–4451.
- 7 G. P. Li, G. Liu, Y. Z. Li, L. Hou, Y. Y. Wang, Z. Zhu, *Inorg. Chem.*, 2016, **55**, 3952–3959.